Nanocomposites of Polyethylene/Polyaniline/Graphite With Special Morphology

Ariane M. Lentz,[1] **Grasiela Gheno,**[1] **Thuany Maraschin,**[2] **José A. Malmonge,**[3] **Nara R. de Souza Basso,**[2] **Naira M. Balzaretti,**[4] **Marcéo A. Milani,**[1] **Griselda B. Galland** (iD)[1]

[1]*Instituto de Química, Universidade Federal do Rio Grande do Sul, Avenida Bento Gonçalves 9500, Porto Alegre 91501-970, Brazil*

[2]*Faculdade de Química, Pontifícia Universidade Católica do Rio grande do Sul, Avenida Ipiranga 6681, 90619-900 Porto Alegre, Brazil*

[3]*UNESP- Univ. Estadual Paulista, Departamento de Física e Química, Campus de Ilha Solteira, 15385-000 Ilha Solteira, SP, Brazil*

[4]*Instituto de Física, Universidade Federal do Rio Grande do Sul, Av. Bento Gonçalves, 9500, Porto Alegre 91570-970, Brazil*

Nanofillers of polyaniline nanofibers (PANI) with graphite oxide (GO) or reduced graphite oxide (rGO) were synthesized and characterized. Four samples of PANI/graphite with 10% and 30% of GO or rGO were obtained. The addition of GO or rGO in PANI nanofibers increased the conductivity and improved the thermal stability of the nanofillers. These nanofillers were used in the *in situ* ethylene polymerization producing PE/PANI/graphite nanocomposites characterized by SEM and TEM, revealing very particular morphologies. PANI/GO or PANI/rGO nanoparticles showed a good dispersion in polyethylene, and an increase in the thermal stability of the final material was observed. POLYM. COMPOS., 39:3645–3655, 2018. © 2017 Society of Plastics Engineers

INTRODUCTION

Polyaniline (PANI) is an intrinsically conductive polymer (ICP) that has attracted considerable attention due to its easy high yield synthesis, low cost monomer, tunable properties, and high environmental stability [1]. There are three isolated forms of polyaniline: leucoemeraldine base (yellow compound), emeraldine base (blue compound), and pernigraniline base (purple compound). The emeraldine salt (green compound) exists in a highly conductive

form [2]. The conjugated π-electron system of PANI is responsible for the electronic conductivity. Nonetheless, its electronic properties can be improved by doping with different types of inorganic charges to develop promising materials [3]. Several studies have shown the influence of the dopant nature and protonation state on the dielectric properties of PANI. The conductivity can be also enhanced using a highly conductive filler as graphite. In recent years, composites based on PANI and graphite have shown scientific and technological potential in several applications [4–8] such as batteries [9, 10], sensors [11], electromagnetic shielding (intelligent packaging) [12], anticorrosive coatings [13], solar cells [14, 15], and supercapacitors [16, 17].

Graphite is formed by a layered structure of hexagonal carbon atoms and, due to its electrical and mechanical properties, it has attracted considerable interest as a filler in polymers. To obtain efficient electrical properties, the layers of graphite, known as graphene, must be separated so they can be dispersed throughout the polymer [18]. Graphite intercalated compounds (GIC's) can be obtained using oxidizing agents in which polar groups move away the layers of graphene [19]. The use of GICs in combination with intrinsically conductive polymers such as PANI increases PANI stability and optimizes its capacitance value [20]. Also, the addition of graphene nanosheets into the polymer matrix can improve the electrical properties of the final compound. Lin et al. [21] prepared and characterized polyaniline/graphene composites and they observed that the conductivity strongly depended on the content of sodium dodecyl sulfate, which was used as a dopant. Graphene oxide is a promising filler for PANI composites because

this material is also capable of enhancing its stability and capacitance [20]. GO not only serves as conductive support but also provides a large surface for the dispersion of the PANI nanoparticles [15, 22]. However, PANI/graphite or PANI/GO nanocomposites do not have a good processability. This handicap could be overcome by dispersing PANI/graphite or PANI/GO nanoparticles in a flexible and high processing matrix. Polyethylene (PE) could be a very good matrix choice due to its low cost, good thermal, mechanical, and optical properties, high resistance to chemicals and excellent processability [21]. Chipara et al. [23] prepared blends of PE and PANI that were mixed and milled together on a two-roller mixer. They observed that the electrical conductivity and mechanical properties of PE/PANI composites depended on the concentration of conductive particles. The increase of PANI content into the PE matrix increased the electrical conductivity but decreased the mechanical properties due to the poor adhesion between PANI particles and the polymeric matrix. The polymerization of ethylene in the presence of PANI nanofibers by *in situ* polymerization was studied recently [24] and it can be a good option for improving the dispersion of the nanoparticles. Recently our research group obtained graphite nanosheet/polyolefins nanocomposites with a good improvement on the Young modulus, crystallization temperature, thermal stability and conductivity using *in situ* polymerization with metallocene catalysts [25]. In this work, the new approach consists in the addition of PANI nanofibers combined with graphene into ethylene by *in situ* polymerization. This system could be a good alternative to improve the electrical conductivity of PANI and to prepare lightweight and easy processable conductive polymeric materials.

Thus, in this work we report the preparation of PANI nanofibers using a modified rapid mixing polymerization procedure in the presence of 10% and 30% of graphite oxide (GO) or reduced graphite oxide (rGO) nanosheets. The effect of the graphite content on the morphology, structure, conductivity and thermal stability of a PANI/graphite nanofiller is discussed. The PANI/graphite particles were used in the *in situ* polymerization of ethylene with a metallocene catalyst to obtain PE/PANI/GO and PE/PANI/rGO nanocomposites. The nanocomposites were characterized by scanning and transmission electronic microscopy and the thermal and electrical properties were also evaluated.

EXPERIMENT

Materials

Graphite flakes were provided by Nacional de Grafite Ltda (Brazil). Nitric acid (P.A. 65%, MERCK), sulfuric acid (P.A. 98%, F.MAIA), potassium chlorate (P.A. 99%, VETEC), hydrochloric acid (P.A. 37%, NEON), ethyl alcohol (P.A. 95%, NUCLEAR), ammonium persulfate (APS, P.A. 98%, VETEC), acetone (P.A., MERCK), and methylaluminoxane (MAO 5 wt% Al solution in toluene,

ALDRICH) were used as received. Aniline (P.A. 99%, SYNTH) was distilled before polymerization.

Synthesis of Graphite Oxide (GO)

The graphite oxide samples were prepared using a modified Staudenmaier method [26, 27]. Nitric acid (45 mL) was added to sulfuric acid (80 mL) in an ice bath and stirred for 1 h. Then, graphite (5 g) and potassium chlorate (55 g) were added while maintaining the temperature and constantly stirring for 20 min. The reaction mixture was stirred for 24 h, and then 600 mL of 10% hydrochloric acid was added. The crude mixture was centrifuged, and the first washing water was removed. Then, the residue was dispersed in water and sonicated for 4 h. A dialysis membrane was used to reach pH 3. The concentration was estimated by gravimetry and dilutions were performed to obtain aqueous suspensions of 0.0149 g/20 mL and 0.034 g/20 mL of GO. The suspension remained in an ultrasonic bath for 4 h.

Reduction of Graphite Oxide (rGO)

The resulting dried graphite oxide was heated in a quartz ampoule up to 1000°C for 10 s. The particles were removed from the ampoule using a solution of 70% aqueous alcohol. The dispersed solution was dried in a furnace at 150°C for 3 h and then weighed. Next, 200 mL of distilled water were added and the suspension was immersed in an ultrasonic bath for 4 h to obtain a good dispersion of the material.

Synthesis of Polyaniline Nanofibers/Graphene Nanofiller

PANI nanofibers were chemically synthesized using a modified rapid mixing polymerization procedure [28, 29]. Distilled aniline (0.6 mL), ammonium persulfate (0.38 g) and 1M aqueous hydrochloric acid solution (20 mL) were transferred to GO (10% or 30% aqueous solution) and stirred at 60°C for 20 s. When the solution began to change to a dark green color, it was allowed to react for an additional 2 h. The product was filtered and washed with distilled water and acetone.

The PANI/rGO compound was synthesized using the same method described above. We obtained 4 nanocomposites samples with concentrations in wt%, described as PANI/GO10 (10% of GO), PANI/GO30 (30% of GO), PANI/rGO10 (10% of rGO), and PANI/rGO30 (30% of rGO). All the nanocomposites were dried sob vacuum before characterization and use as nanofillers in the ethylene polymerization.

Characterization of PANI/Graphite Nanofiller

The PANI/GO and PANI/rGO nanocomposites morphology was analyzed using a FEIInspect F50 and a Field Emission Scanning Electron Microscope. Transmission
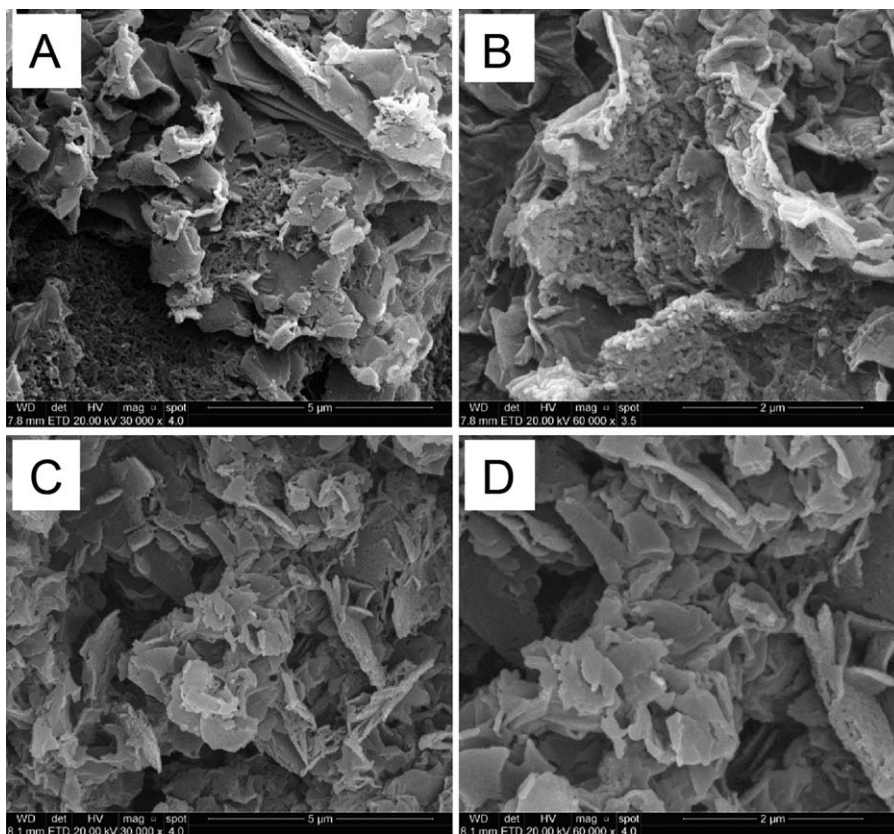
FIG. 1. SEM images of the PANI/GO10 (a and b) and PANI/GO30 (c and d) samples (a and c, bar: 5 μm and b and d, bar: 2 μm).

Electron Microscopy (TEM) measurements were performed using a JEM-1200 EXll microscope. X-ray diffraction (XRD) measurements were carried out on a Rigaku DMAX 2200 diffractometer. Fourier Transform Infrared Spectroscopy (FTIR) spectra were recorded on a Shimatzu FTIR 8300 spectrophotometer in the range of 500–4,000 cm^{-1} at room temperature. The powdered samples (1 mg) were dispersed into tablets with KBr (100 mg) and collected in the transmission mode using 32 scans.

Thermogravimetric analyses (TGA) were conducted under an N$_2$ flow at a heating rate of 20°C.min^{-1} from 25 to 900°C using SDT Q600 Ta Instruments. Raman spectra were recorded on an Olympus microscopy coupled to a Jobin Yvon IHR320 spectrometer attached to a CCD (charged coupled device) detector using a HeNe as the excitation laser (632.8 nm). The acquisition time of 20 s. Electrical conductivity was measured at room temperature on pressed pellets (13.4 mm diameter, < 1 mm thick) using a two-probe method with a model 236 source measure unit from Keithley Instruments. The pellets were made using 700 MPa pressure for 5 min at room temperature. For better electrical contact, circular silver electrodes (9 mm diameter) were painted on both sides of the pellets. The conductivity was obtained using the equation σ=(IxW)/(VxA), where V is the voltage applied to the sample, A is the silver painted area, W is the thickness of the sample and I is the current driven through the sample.

Synthesis of PE/PANI/Graphene Nanocomposites

Nanocomposites PE/PANI/GO and PE/PANI/rGO were prepared by the *in situ* polymerization of ethylene. The catalyst used was bis(cyclopentadyenil)zirconium dichloride (Cp$_2$ZrCl$_2$) and methylaluminoxane (MAO) was used as a cocatalyst. A suspension of the filler in toluene was given an ultrasonic bath for 5 h. Then, MAO (15% in weight of the filler) was added to the ultrasonic bath for an additional 30 min. The reaction was carried out in a 100 mL PARR reactor under 60°C at ethylene pressure of 2.8 bars for 30 min. The amount of filler varied between 1% and 10%.

Characterization of PE/PANI/Graphene Nanocomposites

The nanocomposites PE/PANI/GO were characterized by MEV and TGA in the same conditions described previously. Differential Scanning Calorimetry (DSC) measurements were performed on a TA Q20 instrument under N$_2$ atmosphere. The samples with weights ranged from 7 to 10 mg were in the form of powder such as they were obtained from the polymerization. The samples were
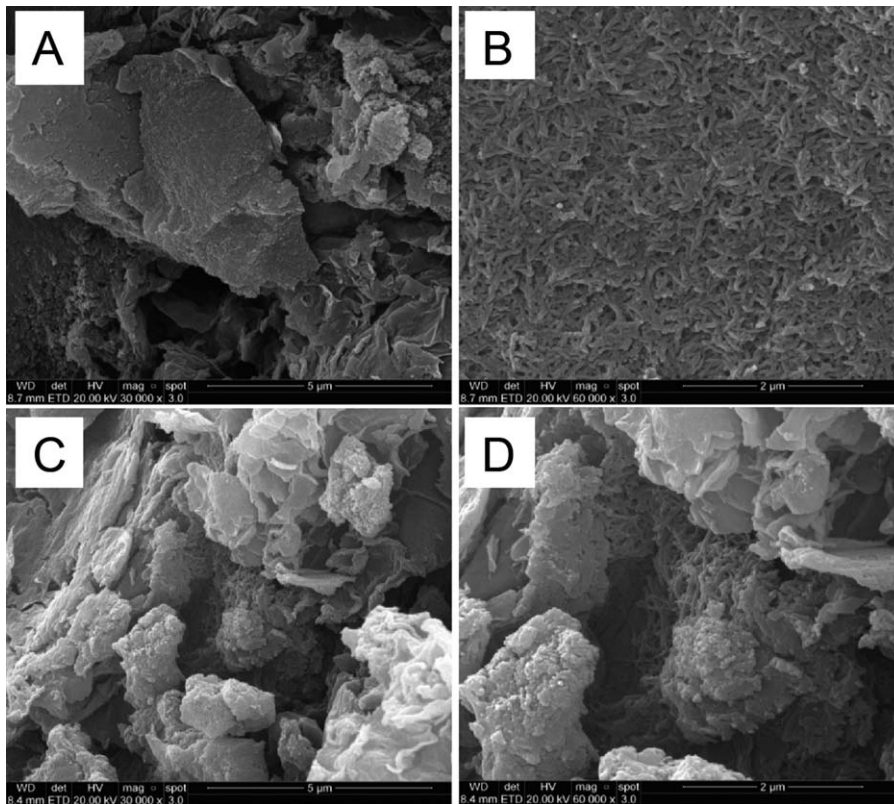
FIG. 2. SEM images of the PANI/GOr10 (a) and (b) and PANI/GOr30 (c) and (d) samples (a and c, bar: 5 μm and b and d, bar: 2 μm).

heated from 25 to 160°C, kept at this temperature for 2 min to erase the thermal history and cooled down to 25°C at a heating/cooling rate of 20°C.min^{-1}. The crystallization temperature (T_c) was taken from the cooling and the melting temperature (T_m) and heat of fusion (ΔH_f) values were taken from the second heating curve. The degree of crystallinity (X_c) was calculated from ΔH_f and using the equation $\Delta H_f \times 100/64.5$ [30].

TEM measurements were performed using a JEOL-1011 microscope. The electrical conductivity was measured using two-probe methods as described previously. A Keithley Instruments voltage source, model 247 and a Keithley Instruments Electrometer, model 610 C, were used for electrical measurements.

RESULTS AND DISCUSSION

PANI/GO Characterization

The aniline polymerization reaction is very simple and fast. The color change of the solution to dark green at the beginning of the polymerization reaction indicates the formation of PANI in its emeraldine salt form. The time required for the color change of the mixture depends on the molar ratio of ammonium persulfate/aniline and the reaction temperature [28]. In this study, emeraldine salt was rapidly obtained using a reaction temperature of 60°C. PANI

nanofillers with 10% and 30% of GO or rGO were synthesized; for higher loads of GO or rGO it was observed the formation of a film that hinder the polymerization of aniline.

Figure 1 shows SEM images of PANI/GO10 and PANI/GO30 nanofillers (SEM images of PANI, GO and rGO are shown in the Supporting Information). It can be observed that PANI is in the form of nanofibers in all cases. Those nanofibers decorate the surface of the GO layers. As expected, a higher ratio of PANI/GO showed a larger amount of PANI nanofibers, as can be seen in Fig. 1a and b. Figure 1c and d show the samples with the lower content of PANI. The nanofibers of PANI presented an average diameter of 62 nm. Figure 2 shows SEM images of PANI nanofillers with rGO. The nanofibers can be seen in both micrographs and the rGO seems to be highly recovered by them, showing a high interaction between both materials. This interaction could be due to π-π stacking [22].

Figure 3 shows TEM images of PANI nanofillers with GO (3A and 3B) and rGO (3C and 3D) for both concentrations. In the micrographs, it can be observed that large sheets of graphene are transparent and entangled with each other. The PANI exhibited the nanofiber morphology. Graphite and PANI nanofibers are present homogeneously distributed in all samples. It is possible to observe a few lines in Fig. 3c and d that may be sheets of aligned graphene layers.
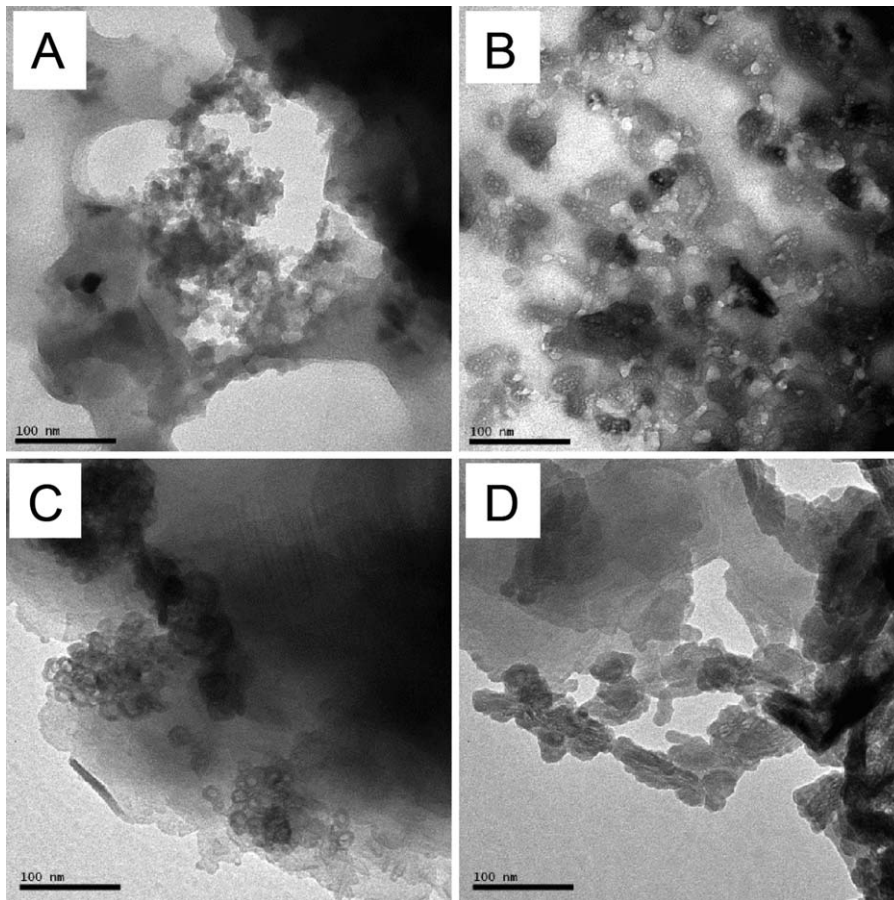
FIG. 3. TEM images of the PANI/GO10 (a), PANI/GO30 (b), PANI/GOr10 (c), and PANI/rGO30 (d) samples (bar: 100 nm).

The TGA curves in Fig. 4 show the thermograms of pure PANI, GO, rGO, PANI/GO, and PANI/rGO nanofillers in both concentrations (10% and 30%), revealing weight loss in several steps (the individual thermograms with their derivates are shown in the Supporting Information). The first step shows mass loss relative to the evaporation of absorbed water molecules and volatiles, such as dopant excess [28]. Pure PANI and rGO loose about 10% of their weight, while GO looses more weight in this step (38% at around 70°C). This could be related to the presence of oxygenated groups that facilitate the adsorption of water molecules on the GO surface. It was also observed that nanocomposites with a higher ratio of oxidized or reduced PANI/graphite presented a slightly higher weight loss (6–7% for PANI/rGO10 and PANI/GO10) than nanocomposites with a higher amount of graphite (4% for PANI/rGO30 and PANI/GO30), probably due to the facility of water absorption by PANI. The second weight loss step at 220°C for pure PANI and at 280°C for PANI/GO nanocomposites was due to the loss of the PANI dopant (HCl) and the oligomers of PANI [21]. GO has an important loss of functional oxygen groups (23%) at this temperature, as well as PANI/GO10 and PANI/GO30 that loose 15% and 21%, respectively. The loss of PANI/rGO nanocomposite is 6–9% of mass,

which is very similar to the weight loss of pure PANI (7%). During the third step, at around 430°C for all samples, the mass loss for PANI is only of 7% and involves the loss of low molecular weight fragments [4]. The weight loss above 430°C can be attributed to the
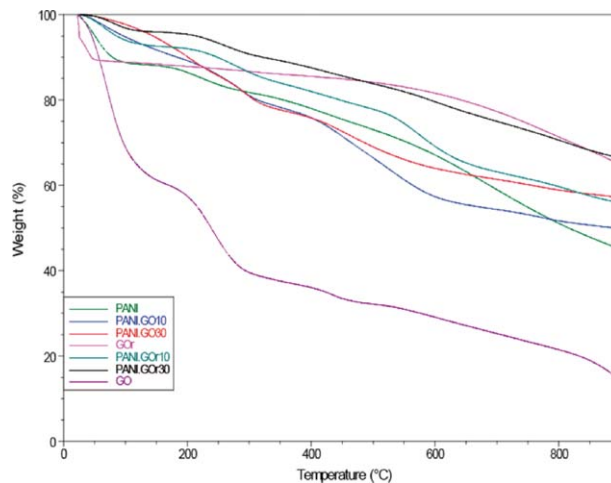

FIG. 4. TGA curves of: pure PANI, PANI/GO10, PANI/GO30, PANI/rGO10, PANI/rGO30, GO, and rGO. [Color figure can be viewed at wileyonlinelibrary.com]
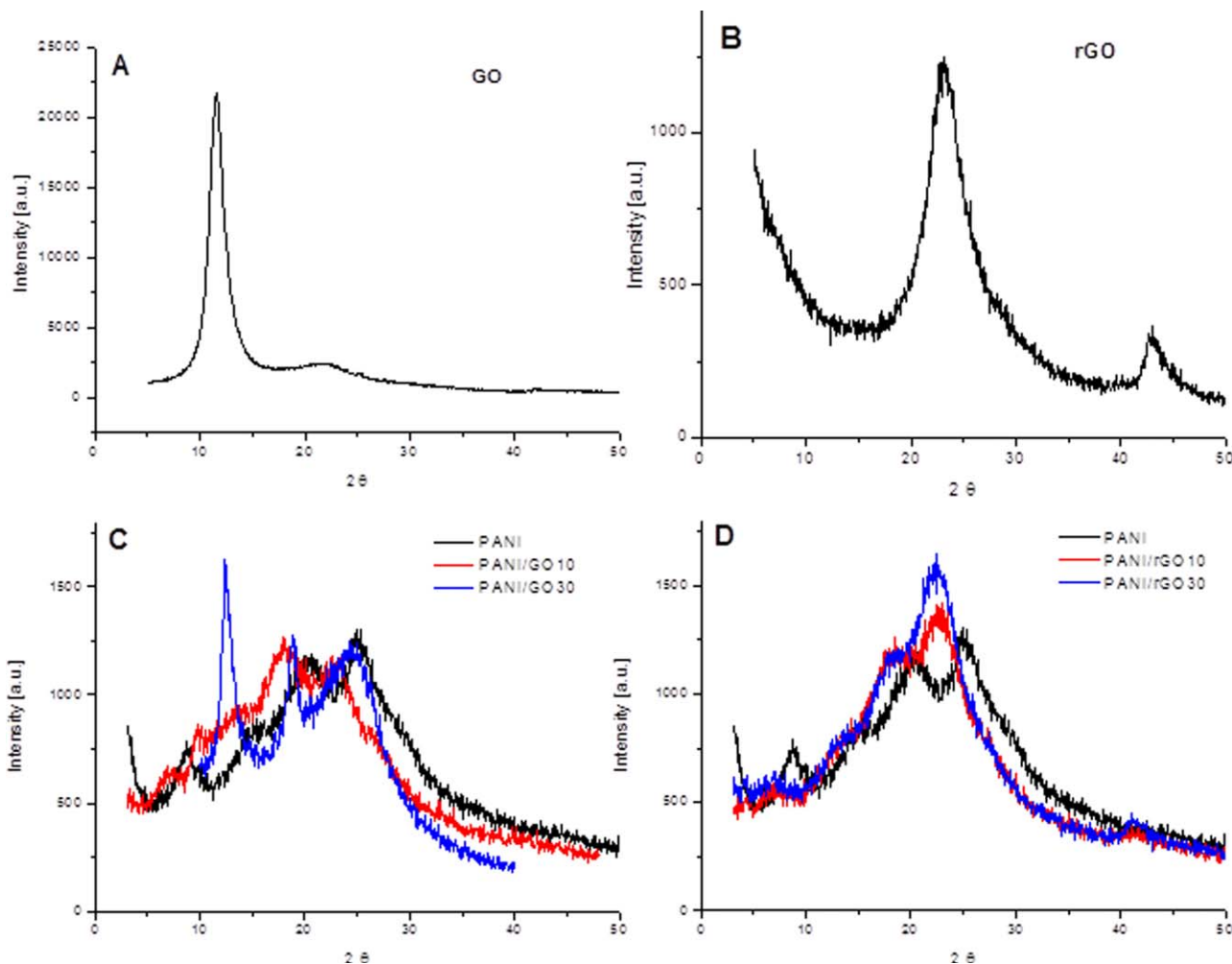
FIG. 5. XRD patterns of: (a) Pure GO; (b) Pure rGO; (c) Pure PANI; PANI/GO10 and PANI/GO30; (d) Pure PANI; PANI/rGO10 and PANI/rGO30. [Color figure can be viewed at wileyonlinelibrary.com]

beginning of the degradation of PANI. Comparing the curves shown in Fig. 4, it is possible to observe that higher amounts of GO or rGO (30%) result in higher thermal stability in the nanocomposites. Also, the thermal stability of the samples containing rGO is higher compared to samples containing GO due to the lower amount of oxygen groups. GO presents several oxygen functional groups in it structure, such as hydroxyl, carbonyl, carboxylic acid and epoxy [31]. When it is reduced at 1,000°C, most of these groups are removed, increasing the stability of the material.

Figure 5 presents the XRD patterns of GO, rGO, PANI, PANI/GO10, PANI/GO30, PANI/rGO10, and PANI/rGO30. Pure GO shows a diffraction at $2\theta = 12°$, corresponding to an interlayer distance of 0.77 nm (calculated using Bragg's Law *Equation* [32]), which is typical of graphite oxide [20]. When GO was reduced to rGO, this signal shifted to $2\theta = 23.0°$, decreasing the distance between graphenes to 0.39 nm due to the elimination of oxygen functional groups. Pure PANI nanofibers show intense peaks at $2\theta = 20.1°$ and $25.0°$ that are

characteristic of the crystalline planes (100) and (110) of the emeraldine salt form, respectively [18, 20]. In both samples of PANI/GO nanofillers, the GO peak was clearly observed around $2\theta = 11.5°$, corresponding to an interlayer distance of 0.72–0.75 nm. In the nanofiller with a higher amount of GO (30%), this peak is much more intense, as it should be expected. For this sample, a well defined peak is observed close to 19° which has not been observed for the other samples and that it can be attributed to a crystalline structure produced by the interaction between PANI and GO. In the nanofiller with rGO it is possible to identify the contributions from PANI and rGO peaks, even though there is an overlap in the region close to 24°.

The FTIR spectra of GO, rGO, PANI, PANI/GO30, PANI/rGO30, PANI/GO10, and PANI/rGO10 in the region of 2,000–600 cm^{-1} are shown in Fig. 6. (The full spectra of these samples are included in the Supporting Information). The characteristic absorption peaks for GO are centered at 3,424, 1,625, and 1,181 cm^{-1} assigned to the stretching of O—H, C=C (the aromatic graphene rings), and C—O
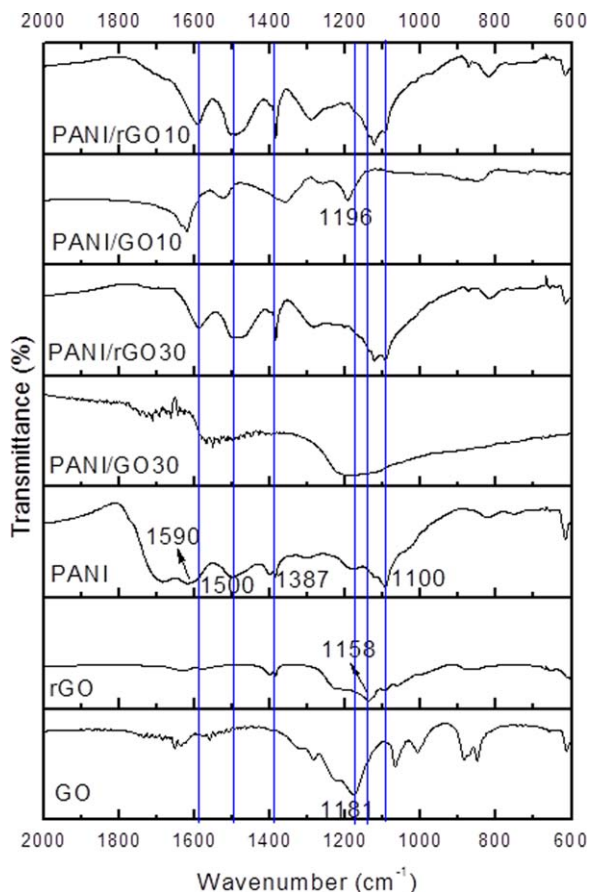
FIG. 6. FTIR spectra of PANI/rGO10, PANIGO10, PANI/rGO30, PANI/GO30, pure PANI, rGO, and GO samples in the region of 2000–600 cm^{-1}. [Color figure can be viewed at wileyonlinelibrary.com]

groups, respectively. The FTIR of pristine PANI shows the absorption bands centered at 1,590, 1,500, 1,387 and around 1,100 cm^{-1} corresponding to the stretching of C=N quinoid rings, C=C of benzenoid rings, C—N of —N—benzenoid—N and C=N of N=quinoid=N—, respectively. The band at 822 cm^{-1} correspond to C—H bending vibration of 1,4-substituted phenyl ring [21]. The FTIR spectrum of the sample with a higher amount of GO (PANI/GO30) is very similar to GO, the PANI bands seems to be masked by the strong GO bands. . This result is consistent with the XRD pattern for this sample, in which the presence of GO is very pronounced. The GO band due to C—O stretching at 1,181 cm^{-1} is also present in the nanocomposites PANI/GO10 and PANI/GO30 but as it can be seen in PANI/GO10 it is shift to 1,196 cm^{-1} suggesting some interaction of GO with PANI. In rGO, this C—O stretching band appears at 1,158 cm^{-1} and it is present also in the nanocomposites PANI/rGO10 and 30 with a slight shift to lower frequencies. The PANI main bands at 1,590, 1,500, and 1,387 cm^{-1} are clearly seen in PANI/rGO10 and PANI/rGO10 nanocomposites, moreover in PANI/GO10 the benzenoid (1500) and C—N (1387) bands are shift to 1,523 and 1,357 cm^{-1}, respectively, suggesting a possible interaction of PANI with GO.

The Raman spectrum of GO, rGO, and nanofillers are shown in Fig. 7. The peaks centered at 1,350 and 1,591 cm^{-1} in the Raman spectrum of GO and rGO samples were attributed to the D band (in-plane vibrations of disordered carbon) and G band (E2g mode) of graphite. In the pristine PANI, characteristic peaks are centered at 1,173, 1,370, and 1,600 cm^{-1}, corresponding to the C—H bending vibration of the benzenoid or quinoid rings, the C—N^{+} stretching vibration that demonstrates that the PANI was in the doped state and C—C stretching vibration of the benzenoid ring, respectively. The peaks at 1,240 and 1,504 cm^{-1} were attributed to the C—N and C=N stretching in the emeraldine state, respectively, suggesting that PANI was in the nanofillers in the conductive state, which is consistent with the presence of the emeraldine color [9]. For all samples, the Raman spectrum of PANI is clearly seen. The contribution of GO or rGO is not distinguishable, even for PANI/GO30 which has distinct results for XRD pattern and FTIR spectrum.

The results obtained for the electrical conductivity of the nanofillers are presented in Table 1. Although there is no significant differences in the experimental values for the nanofillers with GO in comparison with rGO, it can be observed that the incorporation of GO or rGO into PANI nanofibers increased the electrical conductivity of the nanofillers about 6 times, even though GO has a very low electrical conductivity (insulator). This suggest that electrical conductivity of PANI is enhanced due to the
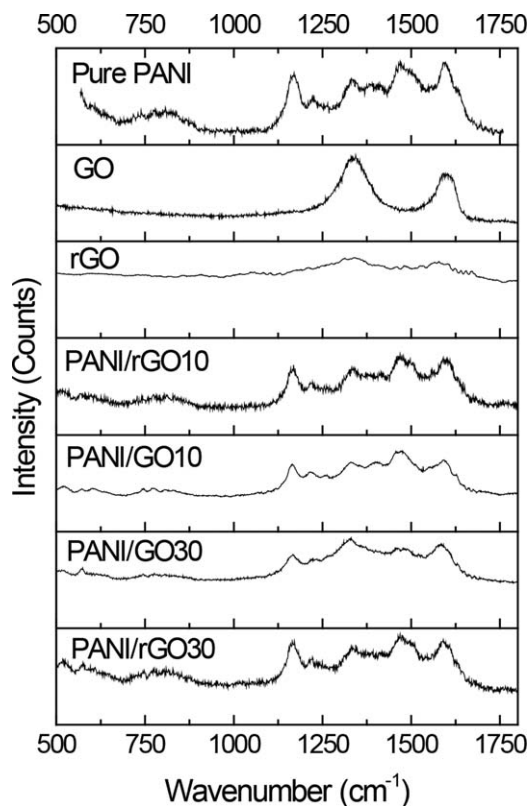

FIG. 7. Raman spectrum of GO, rGO, and nanocomposites PANI/GO and PANI/rGO.

TABLE 1. Electrical conductivity of PANI and nanofillers of PANI with GO and rGO.

Sample	Conductivity (S.cm^{-1})
PANI	0.68×10^{-2}
GO	5.6×10^{-7}
rGO	18.8×10^{-2}
PANIGO10	3.7×10^{-2}
PANIGO30	3.3×10^{-2}
PANIrGO10	4.1×10^{-2}
PANIrGO30	1.8×10^{-2}

interactions between PANI nanofibers with GO and rGO sheets. According to Wang et al. [22], the oxygen groups of GO sheets may interact with PANI through hydrogen bonding and electrostatic interactions, while rGO sheets may interact with PANI mainly by π-π stacking. The SEM images of the nanofillers indicate that graphene sheets provide a flat template for adhesion of as-synthesized PANI [6] increasing the orientation of the nanofibers and enhancing the electrical conductivity.

PE/PANI/GO Characterization

Table 2 shows the results for catalytic activity and thermal properties of *in situ* polymerization of ethylene with nanofillers. It can be observed that the catalytic activity decreases with the increase of the amount of the nanofiller, which is probably due to the presence of the oxygen groups of GO and rGO, which can deactivate the catalyst. Previous works have shown that the addition of small amounts of PANI results in an increase of catalytic activity due to an interaction between PANI and the catalyst [Cp$_2$ZrCl$_2$]/MAO during the *in situ* polymerization of PE [24, 33], in agreement to the results obtained in this work, specially for 1% of the nanofiller PANI/GO10.

Melting temperatures (T_m) showed small variations, within 2–3°C compared to pure PE, without any systematic trend. The degree of crystallization (X_c) of the nanocomposites is systematically higher for samples containing 1% of nanofiller, maybe due to the interaction between PANI and the catalyst, as mentioned above. For larger amounts of nanofillers, this parameter decreases without any specific trend. The crystallization temperature (T_c) increases within 2–6°C for all nanocomposites compared to pure PE, indicating the nucleation power of the filler [34]. The thermal stability obtained from the maximum degradation temperature (T_{max}) from TGA also increases within 5–37°C, being larger for the nanocomposites with a higher amount of GO or rGO (30%). These results suggest that the presence of the nanofiller slows the process of the thermal degradation of polyethylene.

The morphologies of the nanocomposites were studied by SEM and TEM. Figure 8 shows SEM images of PE/PANI/GO10—10% (A), PE/PANI/GO30—7% (B), PE/PANI/rGO10—6% (C), and PE/PANI/rGO30—6% (D), revealing distinct morphologies. For the PE/PANI/GO samples (A and B) it is possible to see some sheets of GO covered by PE. The PE/PANI/rGO10 (Fig. 8c) sample contains an exfoliated, very ordered morphology, suggesting that the nanofiller acted as a template for the growth of the polymer chains.

Figure 9 shows the TEM images of the nanocomposites, revealing a very different morphology between the samples containing GO and rGO. The nanocomposites containing PANI/GO (A and B) present large sheets of PE, suggesting that the polymer used the GO sheets as templates. This morphology is similar to the one presented by metals when the crystallization occurs through a planar growth. Conversely, the nanocomposites with PANI/rGO (C and D) look more like the branches of a

TABLE 2. Catalytic activities and thermal properties of nanocomposites PE/PANI/GO and PE/PANI/rGO.

Sample	Nanofiller (wt.%)	PE Yield (g)	Catalytic Activity[a]	T_m (°C)	T_c (°C)	X_c (%)	T_{max}[b] (°C)
PE	0	5.6	2000	134	114	74	480
PE/PANI/GO10	1.0	8.2	2899	134	116	81	477
	2.0	4.3	1506	134	116	77	488
	4.0	5.3	1817	135	115	74	480
	10.0	3.4	1093	134	117	69	485
PE/PANI/GO30	1.0	4.5	1591	135	117	84	517
	3.0	4.8	1662	136	118	68	512
	6.0	1.8	604	136	118	70	513
	7.0	3.0	996	135	120	71	492
PE/PANI/rGO10	1.0	5.9	2086	135	117	87	481
	3.0	5.7	1975	138	117	69	486
	6.0	2.2	739	136	117	74	485
PE/PANI/rGO30	1.0	6.2	2190	135	118	81	495
	3.0	5.7	1964	135	117	70	491
	6.0	3.9	1312	136	117	65	491

[a]Catalytic activity of polymerization reaction = (kgPE molZr^{-1} bar^{-1} h^{-1}).
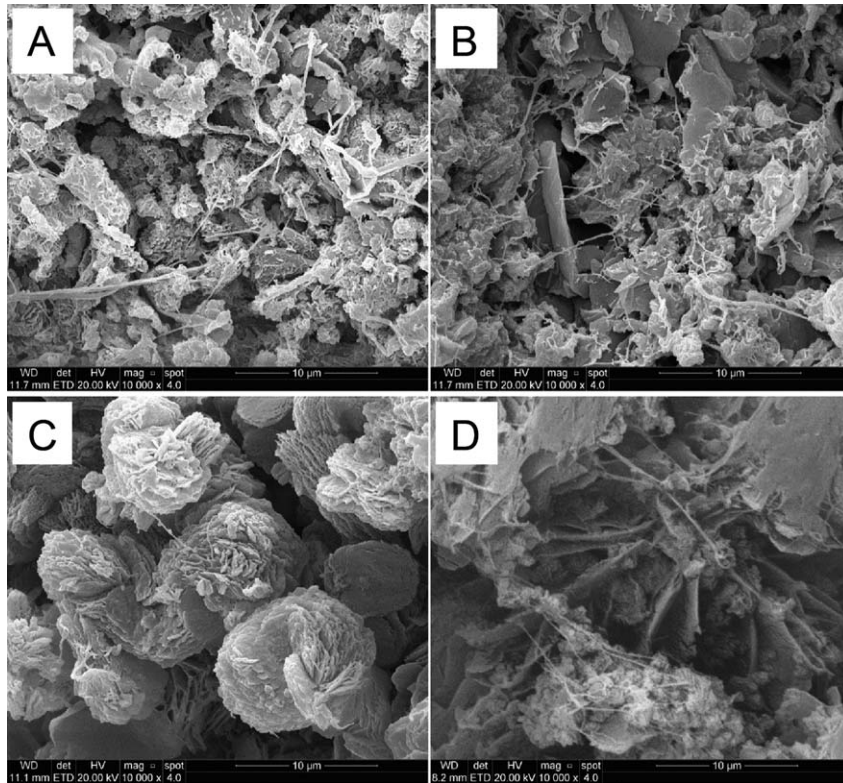[b]Maximum degradation temperature obtained from TGA analysis.

FIG. 8.   SEM images of the nanocomposites PE/PANI/GO10 10 % (a), PE/PANI/GO30 7% (b) PE/PANI/ rGO10 6 % (c), and PE/PANI/rGO30 6% (d) bar: 10 μm).
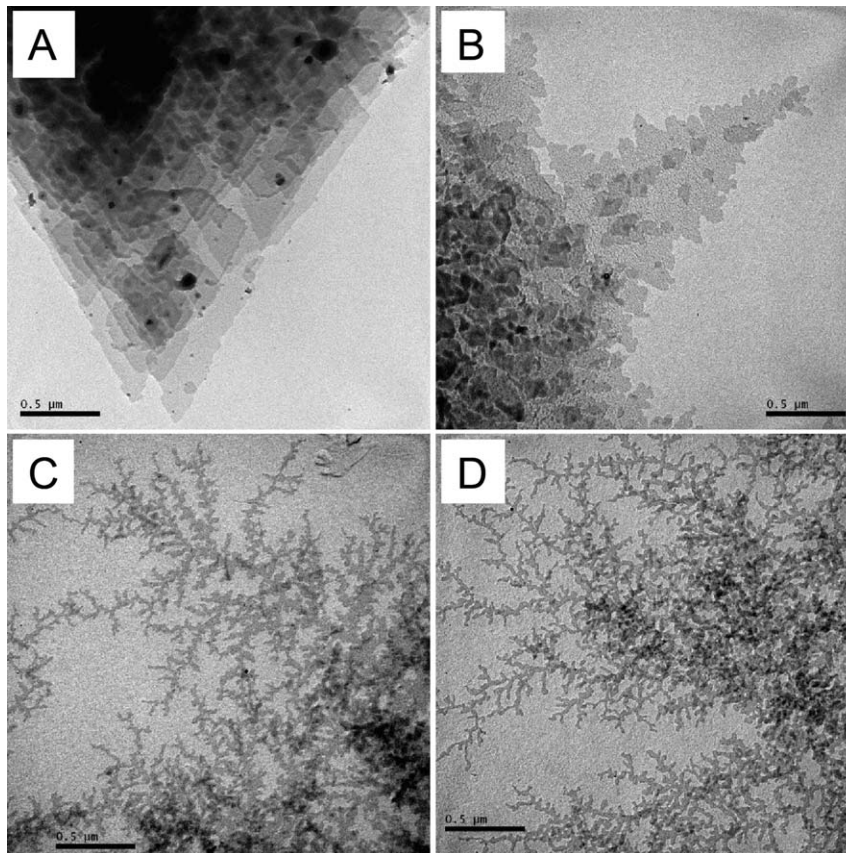

FIG. 9.   TEM images of the nanocomposites PE/PANI/GO10 10 % (a), PE/PANI/GO30 7% (b), PE/PANI/ rGO10 6% (c), and PE/PANI/rGO30 6% (d) (bar: 0.5 μm).

tree. This dendritic morphology is normally presented by metals when their dissipation of heat during solidification is fast [35]. Probably the presence of rGO, that present a higher thermal conductivity than GO, increases the heat dissipation rate producing this dendritic morphology during the crystallization of the nanocomposite.

The nanocomposite PE/PANI/GO10 presented large electrical resistivity and is considered insulator, even for the sample containing 10% of PANI/GO10. Conversely, the nanocomposite PE/PANI/GO30 presented a conductivity of 1.3×10^{-6} S cm^{-1}, compatible with semiconductor materials, with only 7% of PANI/GO30, suggesting that higher amounts of GO in the nanofiller may increase the electrical properties. The nanocomposites PE/PANI/rGO behave as insulators probably due to the maximum amount of filler (6%) obtained in these preparations, which was not enough to achieve the conductivity threshold. This behavior confirms the results of Table 1 that the electrical conductivity occurs mainly through the PANI π-π system but the interaction with GO or rGO sheets through π-π stacking has the synergic effect to enhance conductivity independent on the graphite nanosheet used.

CONCLUSIONS

Nanocomposites of polyaniline with graphene oxide and reduced graphene oxide were easily synthesized by a modified rapid mixing polymerization. TEM and SEM images showed the nanofiber morphology of PANI entangled between the GO or rGO layers, indicating a well dispersed material. The thermal stability was increased by the presence of rGO in the nanofillers. The electrical conductivity of the nanofillers was improved by about 6 times with the addition of GO or rGO compared to pure PANI. PANI/GO and PANI/rGO were used as nanofillers to obtain PE/PANI/GO or PE/PANI/rGO nanocomposites. The good dispersion of the nanofillers in the PE nanocomposite was observed by electronic microscopy. The SEM and TEM images revealed significant differences in morphologies between the polyethylene nanocomposites obtained by PANI/GO or PANI/rGO nanofillers. Nanocomposites with GO resemble layered materials and with rGO resemble branches of a tree. Electrical conductivity seems to occur mainly through the PANI polymer but the interaction with GO or rGO sheets has a positive effect on it. Polyethylene nanocomposite with 7% of PANI/GO30 as filler showed potential as flexible semiconductor.

ACKNOWLEDGMENT

REFERENCES

1. S. Bhadra, D. Khastgier, N.K. Singha, and J.H. Lee, *Prog. Polym. Sci.*, **34**, 783 (2009).

2. P. Barta, Th. Kugler, W.R. Salaneck, A.P. Monkman, J. Libert, R. Lazzaroni, and J.L. Brédas, *Synth. Met.*, **93**, 83 (1998).

3. S. He, Q. Wang, Y. Yu, Q. Shi, L. Zhang, and Z. Chen, *Biosens. Bioelectron.*, **68**, 462 (2015).

4. G. Gheno, N.R.S. Basso, and R. Hübler, *Macromol. Symp.*, **299/300**, 74 (2011).

5. E.A. Özerol, B.F. Senkal, and M. Okutan, *Microelectron. Eng.*, **146**, 76 (2015).

6. J. Xiang, and L.T. Drzal, *Polymer*, **53**, 4202 (2012).

7. X.S. Du, M. Xiao, and Y.Z. Meng, *Eur. Polym. J.*, **40**, 1489 (2004).

8. X.S. Du, M. Xiao, and Y.Z. Meng, *J. Polym. Sci., Part B: Polym. Phys.*, **42**, 1972 (2004).

9. F. Ye, B. Zhao, R. Ran, and Z. Shao, *J. Power Sources*, **290**, 61 (2015).

10. K. Ghanbari, M.F. Mousavi, and M. Shamsipur, *Electrochim. Acta*, **52**, 1514 (2006).

11. I. Fratoddi, I. Venditti, C. Cametti, and M.V. Russo, *Sens. Actuators B*, **220**, 534 (2015).

12. P. Modak, S.B. Kondawar, and D.V. Nandanwar, *Procedia Mater. Sci.*, **10**, 588 (2015).

13. L.H.E. Santos, J.S.C. Branco, I.S. Guimarães, and A.J. Motheo, *Surf. Coat. Technol.*, **275**, 26 (2015).

14. A. Bahramian and D. Vashaee, *Sol. Energy Mater. Sol. Cells*, **143**, 284 (2015).

15. G. Wang, X. Wei, and Z. Shuping, *Electrochim. Acta*, **66**, 151 (2012).

16. B. Song, L. Li, Z. Lin, Z.K. Wu, K.S. Moon, and C.P. Wong, *Nano Energy*, **16**, 470 (2015).

17. Q.F. Lü, G. Chen, T.T. Lin, and Y. Yu, *Compos. Sci. Technol.*, **115**, 80 (2015).

18. J. Zhu, M. Chen, H. Qu, X. Zhang, H. Wei, Z. Luo, H.A. Colorado, S. Wei, and Z. Guo, *Polymer*, **53**, 5953 (2012).

19. R.K. Layek, and A.K. Nandi, *Polymer*, **54**, 5087 (2013).

20. Y. Jin and M. Jia, *Synth. Met.*, **189**, 47 (2014).

21. Y.-C. Lin, F.-H. Hsu, and T.-M. Wu, *Synth, Met.*, **184**, 29 (2013).

22. H. Wang, Q. Hao, X. Yang, L. Lu, and X. Wang, *Appl. Mater. Interfaces*, **2**, 821 (2010).

23. M. Chipara, D. Hui, P.V. Notingher, M.D. Chipara, K.T. Lau, J. Sankar, and D. Panaitescu, *Compos. Part B: Eng.*, **34**, 637 (2003).

24. A.P. Graebin, L. Bonnaud, O. Persenaire, P. Dubois, Z.N. Rocha, and N.R.S. Basso, *Mater. Res.*, **18**, 121 (2015).

25. M.A. Milani, R. Quijada, N.R.S. Basso, A.P. Graebin, and G.B. Galland, *J. Polym. Sci. Part A: Polym. Chem.*, **50**, 3598 (2012).

26. L. Staudenmaier, *Ber. Dtsch. Chem. Ges.*, **31**, 1481 (1898).

27. M. Herrera-Alonso, A.A. Abdala, M.J. McAllister, I.A. Aksay, and R.K. Prud'homme, *Langmuir*, **23**, 10644 (2007).

28. J. Qiang, Z. Yu, H. Wu, and D. Yun, *Synth. Met.*, **158**, 544 (2008).

29. W. He, W. Zhang, Y. Li, and X. Jing, *Synth. Met.*, **162**, 1107 (2012).

30. K. Soga, *Makromol. Chem.*, **190**, 995 (1989).

31. S. Pei and H.M. Cheng, *Carbon*, **50**, 3210 (2012).

32. J.B. Aladekomo and R.H. Bragg, *Carbon*, **28**, 897 (1990).

33. N.R.S. Basso, F. Oliveira, A.P. Graebin, C.S. Moura, F.C. Fim, G.B. Galland, L. Bonnaud, O. Murariu, and P. Dubois, *J. Appl. Polym. Sci.*, **131**, 41197 (2014).

34. G. Pavoski, T. Maraschin, M.A. Milani, D.S. Azambuja, R. Quijada, C.S. Moura, N.S. Basso, and G.B. Galland, *Polymer*, **81**, 79 (2015).

35. D.R. Askeland and P.P. Phulé, Ciência e Engenharia dos Materiais, Cengage Learning (Eds), São Paulo, Brazil, 246 (2008).